BAREKENG: Journal of Mathematics and Its Applications
December 2025 Volume 19 Issue 4 Page 2661–2678
P-ISSN: 1978-7227 E-ISSN: 2615-3017
https://doi.org/10.30598/barekengvol19iss4pp2661-2678

NUMERICAL ANALYSIS OF BLOOD VESSEL CONSTRICTION DUE TO ATHEROSCLEROSIS DISEASE USING FINITE VOLUME METHOD

Arif Fatahillah[1*], Umi Mubarokah[2], Rafiantika Megahnia Prihandini[3], Edy Wihardjo[4], Robiatul Adawiyah[5], Saddam Hussen[6], Lioni Anka Monalisa[7]

[1,2,3,4,5,6,7]*Mathematics Education Study Program, Faculty of Teacher Training and Education, Universitas Jember*
Jln. Kalimantan No. 37, Kampus Tegalboto, Jember, Jawa Timur, 68121, Indonesia

*Corresponding author's e-mail: * **fatahillah767@gmail.com***

Article History:
Received: 12th February 2025
Revised: 18th March 2025
Accepted: 10th June 2025
Available online: 1st September 2025

Keywords:
Atherosclerosis;
Coronary Artery;
Finite Volume Method;
SIMPLE.

ABSTRACT

Atherosclerosis is a leading cause of coronary heart disease. This study analyses how elliptically shaped stenoses alter blood-flow velocity in coronary arteries. The governing equations are discretised with the finite-volume method, coupling pressure and velocity through the SIMPLE (Semi-Implicit Method for Pressure-Linked Equations) algorithm and accelerating convergence with the Successive Over-Relaxation (SOR) technique. A weighted Gauss–Seidel iteration whose over-relaxation factor ($\omega = 1.7$ in this work) damps low-frequency error modes, cutting the number of iterations needed for residuals to fall below 10^{-4} by roughly 40 % compared with the standard Gauss–Seidel scheme. Simulations of 30 %, 50 %, and 70 % constrictions were carried out in MATLAB R2013a and ANSYS Fluent. Quantitative and qualitative cross-validation of the two software packages confirmed consistent velocity and pressure fields, though minor discrepancies arose from differing numerical schemes and model assumptions, underscoring the need for experimental verification. The highest centre-line velocity occurred at 70 % stenosis—0.72075 m/s *in MATLAB versus 0.90* m/s *in Fluent—while the lowest was recorded at 30 %. Velocity–pressure profiles showed that increasing inlet velocity or degree of narrowing elevates velocity but decreases pressure, with the largest drop (11492.4* Pa *in MATLAB; 11747.32* Pa *in Fluent) again at 70% stenosis. Study limitations include modelling blood as a Newtonian fluid and idealising arterial geometry; future work should incorporate non-Newtonian rheology and patient-specific shapes to enhance physiological accuracy.*

How to cite this article:

A. Fatahillah, U. Mubarokah, R.M. Prihandini, E. Wihardjo, R. Adawiyah, S. Hussen, and L. A. Monalisa, "NUMERICAL ANALYSIS OF BLOOD VESSEL CONSTRICTION DUE TO ATHEROSCLEROSIS DISEASE USING FINITE VOLUME METHOD," *BAREKENG: J. Math. & App.*, vol. 19, iss. 4, pp. 2661-2678, December, 2025.

Journal homepage: *https://ojs3.unpatti.ac.id/index.php/barekeng/*
Journal e-mail: *barekeng.math@yahoo.com; barekeng.journal@mail.unpatti.ac.id*

Research Article · Open Access

1. INTRODUCTION

Heart disease is one of the leading causes of death worldwide, including in Indonesia. According to data from the Global Burden of Disease and IHME (Institute for Health Metrics and Evaluation), coronary heart disease accounts for a significant number of deaths. Recent data from the WHO (World Health Organization) shows that in 2021, heart disease was responsible for about 17.8% of total deaths in the country. The disease is estimated to cause more than 470.000 cases of deaths each year [1]. This figure shows that the prevalence of heart disease continues to increase every year and is a serious concern for the public health sector. One of the main causes of coronary heart disease is atherosclerosis, which is a condition where fatty plaques, cholesterol, and other substances build up in the artery walls.

Atherosclerosis is a medical condition in which the walls of arteries become hardened and thickened. Complications caused by atherosclerosis account for nearly 50% of deaths in developed countries [2]. Atherosclerosis is a major contributing factor to vascular disease worldwide. In developing countries, especially in regions such as Eastern Europe and Asia, a significant increase in atherosclerosis disease has been reported [3]. Atherosclerosis is the loss of connective tissue flexibility and the inability of smooth muscle to relax in blood vessels, resulting in large arteries and the aorta being unable to carry large amounts of blood to the heart [4]. This process causes plaque to build up on the blood vessel walls, resulting in abnormal narrowing of the blood vessels known as stenosis [5]. The plaque is hardened by calcium deposits in the artery, which makes the artery lining rough and obstructs the lumen of the blood vessel. This condition triggers thrombosis, which causes the artery to become blocked and triggers a heart attack if it occurs in the blood vessels of the heart. The narrowing of the arteries causes the flow of blood and essential supplements to decrease. Arteries that are deprived of blood and oxygen increase the risk of stroke, heart failure, and heart attack [6]. The population at risk of atherosclerosis disease amounted to 29.2% of a total of 22,093 samples across Indonesia, which had a significant impact on mortality [7]. The main factors that lead to atherosclerosis include high blood pressure, diabetes, high cholesterol levels and triglyceride levels, and unhealthy lifestyles, such as smoking and physical inactivity.

The case of blood vessel constriction can be modeled using a computer simulation. CFD (Computational Fluid Dynamics) is a tool to understand and analyze blood flow dynamics. CFD is a software computer program used to model heat, mass flow, and chemical reactions that occur during thermal processes [8]. In CFD, a mathematical approach is used to describe the behavior of blood flow inside blood vessels, which includes the analysis of parameters such as blood flow velocity and pressure. CFD simulation provides an efficient, cost- and time-saving solution for understanding blood flow disorders caused by blood vessel constriction. It is effective for quickly analyzing blood flow conditions, without the need for expensive and time-consuming physical experiments [9]. CFD is an effective method for numerical modeling and analysis of fluid flow, based on the Navier-Stokes equations that describe the behavior of fluid flow in a given region [10]. The Navier-Stokes equations can be solved using several methods, such as the finite volume method, finite difference method, and finite element method.

The finite volume method is a numerical approach used in solving various problems, including the case of fluid flow. The finite volume method was developed from the finite difference method, with the advantage of maintaining the conservation of mass, momentum, and energy during the discretization process. It calculates fluxes at the boundaries of the control volume and guarantees that the relevant physical properties are preserved in each computational step [11]. The finite volume method is considered a very effective discretization technique for numerical simulations as it is able to provide a very high level of accuracy [12]. The use of the finite volume method in software enables accurate and efficient simulation of fluid flow, as well as analysis of complex interactions between various physical phenomena [13]. Therefore, this research aims to create a script to solve fluid dynamics problems using the Navier-Stokes equations, especially the fluid flow problem of elliptical blood vessel constriction in coronary arteries.

This research employs the finite-volume method (FVM) together with the SIMPLE pressure–velocity coupling scheme and the Successive Over Relaxation (SOR) linear solver. FVM is selected rather than the finite difference method (FDM) or finite element method (FEM) because its cell-integral formulation enforces local conservation of mass, momentum, and energy by construction, a property that is crucial for capturing the steep pressure and wall shear stress gradients that develop inside arterial stenoses. In addition, FVM handles complex, curved vessel geometries more naturally than the structured grids typically required by FDM, while avoiding the high computational cost and stabilization terms often needed in FEM for incompressible, non-Newtonian flows. The control volume approach also integrates seamlessly with the

SIMPLE algorithm, which was originally developed in an FVM framework, ensuring stable coupling between velocity and pressure fields. Accordingly, the computational domain is discretized into elliptical control volumes that follow the constricted vessel wall; fluxes across each cell face are evaluated so that the Navier–Stokes equations augmented by the Carreau non-Newtonian viscosity model are satisfied in every volume element. This combination of strict conservation, geometric flexibility, and algorithmic compatibility makes FVM the most efficient and accurate choice for simulating blood flow in the stenosed arterial segment studied here.

Coronary artery narrowing is a condition where cholesterol and triglyceride fats accumulate in the arteries, which can cause blood flow to the heart muscle to decrease or stop, thus disrupting the work of the heart **[14]**. Coronary artery narrowing occurs when the supply of oxygen and nutrients that arteries should supply to body tissues is obstructed. The coronary arteries function to provide oxygen and nutrients vital for the heart muscle to maintain optimal performance. Blocked coronary arteries lead to coronary heart disease **[15]**. High blood pressure makes the atherosclerotic plaque crack and become several fragments. Loose plaque fragments can cause blood flow blockage and trigger a heart attack **[16]**. Hussain, Dar, Cheema, Tag-eldin, and Kanwal conducted research in the form of simulations for blood vessel constriction problems formed based on density, viscosity, and thermal conductivity in three types of stenosis, namely triangular, elliptical, and trapezoidal stenosis. The approach used in the study involves solving partial differential equations using the finite element method **[17]**. Blood vessel constriction, or stenosis, is a pathological condition characterized by a reduction in the vessel diameter, significantly affecting blood flow and potentially leading to cardiovascular diseases such as atherosclerosis and ischemia **[18]**. Numerous numerical studies have been conducted to understand the hemodynamic changes caused by stenosis and their impact on the vessel wall. **[19]** performed hemodynamic analysis of stenosed arteries using computational fluid dynamics (CFD), demonstrating the relationship between the degree of narrowing and the distribution of pressure and blood flow velocity. Additionally, **[20]** employed a non-Newtonian fluid model to simulate blood flow in stenosed vessels, highlighting the importance of variable blood viscosity on flow patterns and the potential formation of recirculation zones. These studies deepen the understanding of the geometric and fluid properties involved in stenosis pathology and support the development of more effective diagnostic and therapeutic methods.

Then, to obtain the velocity and pressure components, the SIMPLE (Semi-Implicit Method for Pressure-Linked Equations) discretization technique is applied. SIMPLE is a widely used algorithm for solving the Navier-Stokes equations by iteratively coupling velocity and pressure fields to achieve mass conservation and pressure accuracy **[21]**. The method starts by solving the momentum equations to estimate velocity, followed by a pressure correction step to refine pressure and velocity fields until convergence. Although methods like SIMPLEC offer improved accuracy and faster convergence, SIMPLE is chosen in this study due to its robustness and simplicity, which are sufficient for the scale and objectives of the current blood vessel constriction modeling. To further enhance convergence speed, the SOR method is employed.

In this research, a simulation script for elliptical blood vessel constriction is developed using MATLAB software (MATLAB R2013a **[22]**). MATLAB is a programming language widely used to analyze data, develop and implement algorithms, and visualize data **[23]**. Unlike many previous studies that primarily use commercial CFD tools, this research presents a customizable MATLAB-based model that offers flexibility in parameter tuning and greater transparency in simulation processes. MATLAB was chosen because of its ease of use, high-quality visualization, and numerical stability. The script calculates flow velocity and pressure distribution in blood vessels and visualizes the results graphically. To validate the accuracy of the MATLAB simulation, results are compared with those from Ansys Fluent, a well-established software for simulating complex blood flow geometries requiring high precision. Ansys Fluent is known for realistic modeling, efficient discretization, and intuitive visualization. Several parameters were tested in the MATLAB script to ensure its validity. This study fills the gap in affordable, open-access simulation tools for cardiovascular fluid dynamics and aims to provide practical insights to support prevention and treatment strategies for patients with coronary artery disease. Additionally, the developed script framework can be extended to simulate other fluid dynamics problems governed by the Navier-Stokes equations, broadening its applicability in biomedical engineering and related fields.

2. RESEARCH METHODS

The method used in the numerical analysis of blood vessel constriction due to atherosclerosis disease is simulation research. Simulation research is a type of research that aims to get an overview through a simple system model by performing manipulations to produce effects that are close to real conditions [24]. Simulation aims to analyze data and produce information that is interpreted to ensure the information produced is relevant to the problem [25].

Mathematical modeling is the process of constructing and developing mathematical models to describe and solve problems [26]. Mathematical modeling in this case is based on the mass continuity equation and the momentum equation. The Navier-Stokes equation can be written as follows.

$$\nabla \cdot u = 0 \tag{1}$$

$$\frac{\partial u}{\partial t} + \nabla \cdot uu + \nabla P = \frac{1}{Re}\nabla^2 u \tag{2}$$

Where u is velocity (m/s), P is pressure (Pa), Re is Reynolds number, and ∇ is the nabla operator.

In this study, the narrowing of blood vessels occurs in the left coronary artery, which can be seen in Figure 1 and Figure 2. The velocity value in a steady state [26] and the $\hat{R}$ value [6] are as follows.

$$u = 2u_{avg}\left(1 - \frac{r^2}{\hat{R}}\right) \tag{3}$$

$$\hat{R} = \left[R - \delta sin\left(\pi\left(z - \frac{h}{L}\right)\right)\right]\Omega(t) \tag{4}$$

Where u is the velocity (m/s), u_{avg} is the average velocity (m/s), $\hat{R}$ is the radius of the stenosed artery (m), z is the position in the blood vessel, h is the position of the blood vessel constriction (m), L is the length of the blood vessel (m) and δ is the highest depth of the stenosis (m). The equation of blood flow in coronary arteries can be obtained by substituting the external force parameter into Equation (2). So, the general equation for blood flow in blood vessels due to atherosclerosis disease can be written as follows:

$$\nabla \cdot u = 03 \tag{5}$$

$$\frac{\partial u}{\partial t} + \frac{\partial 2u_{avg}\left(1 - \dfrac{r^2}{\left[R - \delta sin\left(\pi\left(z - \frac{h}{L}\right)\right)\right]\Omega(t)}\right)u}{\partial x} = \frac{1}{\rho}\left(-\frac{\partial P}{\partial x} + \frac{\partial}{\partial x}\left(\mu\left[\frac{\partial^2 u}{\partial x^2}\right]\right)\right) \tag{6}$$

Where u is the velocity (m/s), u_{avg} is the average velocity (m/s), $\hat{R}$ is the radius of the stenosed artery (m), z is the position in the blood vessel, h is the position of the blood vessel constriction (m), L is the length of the blood vessel (m), and μ is the dynamic viscosity of the fluid (Pa.s).

The model used in this study is a model formed based on density, viscosity, and thermal conductivity through the arterial constriction region. The shape of the blood vessel constriction in this study is an elliptical blood vessel.

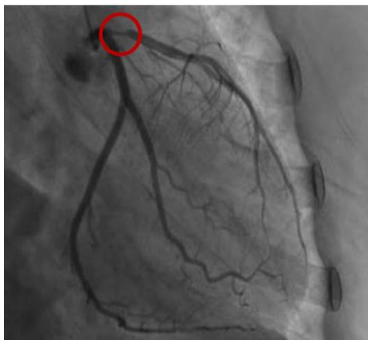

Figure 1. Angiography of Atherosclerosis of the Coronary Arteries [27]

The boundary conditions for the elliptical blood vessel constriction used in this study are as follows

$$\hat{R}(x,t) = \begin{cases} \left[R - \delta \sin\left(\pi\left(\frac{z-h}{L}\right)\right)\Omega(t) \quad h \le z \le h+L\right] \\ [R]\Omega(t), \text{otherwise} \end{cases}$$

With $\Omega(t) = 1 - (\cos \omega t - 1)e^{-i\omega t}$. The piece-wise definition of $\hat{R}(x,t)$ describes how the local hydraulic-resistance coefficient of the artery is modulated along its axis and over the cardiac cycle. Within the stenosed segment that begins at the axial position $z = h$ and extends a length L downstream ($h \le z \le h + L$), the baseline resistance R is reduced by a sinusoidal indentation whose amplitude is the stenosis depth δ; mathematically, this is expressed as $R - \delta \sin\left(\pi\left(\frac{z-h}{L}\right)\right)$. The sine term produces a smooth, symmetric narrowing that reaches its maximum (greatest reduction in lumen radius, hence highest resistance) at the constriction's midpoint and tapers to the healthy value at its ends. This spatial profile is multiplied by the pulsatile modulation Ω(t), a dimensionless time function (e.g., representing systole–diastole variation) that scales the resistance throughout the cardiac cycle. Outside the stenosis ($z < h$ or $z > h + L$) the vessel retains its normal resistance R, again modulated only by Ω(t). Thus, the equation captures both the geometric effect of a localized, sinusoid-shaped stenosis and the temporal fluctuation of flow resistance due to pulsatile blood pressure. In this study, numerical modeling to solve **Equation (5)** and **Equation (6)** above is performed utilizing the finite volume method with SIMPLE discretization and SOR approach.

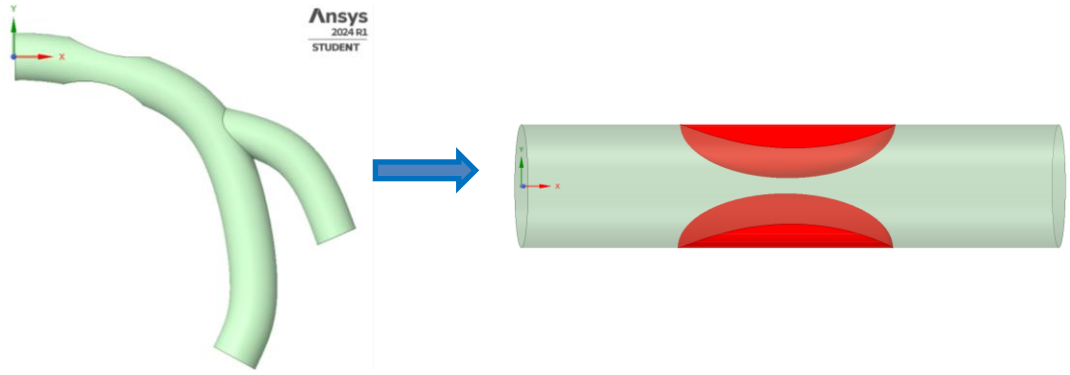

Figure 2. Narrowing Model Reconstruction from Angiography Results

2.1 SIMPLE (Semi-Implicit Method for Pressure-Linked Equations) Discretization

The momentum equation is solved to obtain an estimate of the velocity by assuming initial guesses u^* and P^*. The velocity component u parallel to the x −axis and the pressure component P are assumed with.

$$(u_n^*) = 1 \tag{7}$$
$$(P_n^*) = 0 \tag{8}$$

Then find the value of (u_{n+1}^*) by ignoring the value of (P_n^*) obtained using **Equation (6)**, thus obtaining the system of linear equations below

$$(u^*{}_{n+1})_i = (u_n)_i + \Delta t \left(\left(2u_{avg} \left(1 - \frac{r^2}{\left[R - \delta sin\left(\pi\left(z - \frac{h}{L}\right)\right)\right]\Omega(t)} \right) \right) (u_n)_{i+1} \right.$$
$$\left. - \frac{1}{2\Delta x} \left[- \left(2u_{avg} \left(1 - \frac{r^2}{\left[R - \delta sin\left(\pi\left(z - \frac{h}{L}\right)\right)\right]\Omega(t)} \right) \right) (u_n)_{i-1} \right] + \frac{1}{\rho}\mu \left(\frac{(u_n)_{i+1} - 2(u_n)_i + (u_n)_{i-1}}{(\Delta x)^2} \right) \right) \tag{9}$$

Next, the pressure correction equation is used to correct the pressure using the Poisson equation with respect to the mass equation again. Readjusting the $(n + 1)$ condition to the transient velocity. **Equation (5)** can be written as follows.

$$\frac{(u_{n+1})_{i+1} - (u_{n+1})_{i-1}}{2\Delta x} = 0 \tag{10}$$

Poisson equation.

$$\nabla^2 P = \frac{1}{\Delta t}\nabla(u_n)_i \tag{11}$$

Solve **Equation (11)** to obtain the value of the pressure component. The left segment, $\nabla(u_n)_i$ is called the divergence equation with a temporary velocity component value. Then the divergence equation is written using finite differences as follows.

$$\nabla(u_n)_i = \frac{(u_{n+1})_{i+1} - (u_{n+1})_{i-1}}{2\Delta x} \tag{12}$$

The pressure component is rewritten using a second-order finite difference as follows.

$$\nabla^2 P = \frac{(P_n)_{i+1} - 2(P_n)_i + (P_n)_{i-1}}{(\Delta x)^2} \tag{13}$$

Then **Equation (12)** and **Equation (13)** are substituted into **Equation (11)**, so that the temporary pressure value is obtained as follows.

$$(P_n)_i = \left[\frac{(P_n)_{i+1} + (P_n)_{i-1}}{(\Delta x)^2} - \frac{1}{\Delta t}\nabla(u_n)_i\right]\left[\left(\frac{(\Delta x)^2}{-2}\right)\right] \tag{14}$$

Where $(P_n)_i$ pressure at node i and time level n (Pa), u_n is the velocity component at time level n (m/s), Δx is uniform grid spacing in the axial x-direction (m), Δt is the time-step size between levels n and $n+1$ (s)

2.2 SOR (Successive Over Relaxation) Method

A method that can be used to accelerate the convergence of **Equation (14)** is the SOR method. The equation of the SOR method is as follows.

$$(P_n)_i = (1-\omega)(P_{n-1})_i + \omega(P_n)_i \tag{15}$$

Where ω is the relaxation parameter. Because we use over relaxation, $\omega > 1$.

Next, create a condition where the pressure value is below the maximum value of the tolerance. The tolerance used is 10^{-7}, with the absolute maximum of the pressure $|(P_n)_i - (P_{n-1})_i|$. The condition to be met is $|(P_n)_i - (P_{n-1})_i| < 10^{-7}$. If this condition is met, then the process is stopped (STOP). Otherwise, the pressure value is updated as $(P_n)_i = (P_{n-1})_i$, and the iteration continues using the SOR method to obtain a new pressure value. Additionally, to prevent infinite iterations in case of non-convergence, a maximum number of iterations is set to 500. The maximum iteration limit of 500 was chosen based on both empirical evidence and standard practices in computational fluid dynamics. In all simulation cases, convergence was achieved within fewer than 500 iterations, indicating that this limit is sufficient to ensure solution accuracy while preventing excessive computation time. Similar iteration limits have been recommended in foundational CFD literature to balance convergence reliability and computational efficiency **[11]**.

The velocity correction is obtained by calculating the relationship between the velocity component and the separation pressure component, as in the previous step.

$$\frac{(u_{n+1})_i - (u_n)_i}{\Delta t} = -\frac{(P_n)_{i+1} + (P_n)_{i-1}}{2\Delta x} \tag{16}$$

Since we want the velocity correction at the time of the-$n+1$ condition, the velocity component at the n condition is assumed to be zero. Then substitute it into **Equation (16)**, so that the velocity component correction is obtained as follows.

$$(u_{n+1})_i = -\Delta t\left(\frac{(P_n)_{i+1} + (P_n)_{i-1}}{2\Delta x}\right) \tag{17}$$

Update all component values.

Pressure component

$$(P_{n-1})_i = (P_n^*)_i + (P_n)_i \tag{18}$$

Velocity component

$$(u_{n-1})_i = (u_n^*)_i + (u_n)_i \tag{19}$$

Table 1. Constraints on Blood Flow

Name	Symbol	Value
Thermal Conductivity	k	$0.492\ \mathrm{W/mk}$
Blood Density	ρ	$1063\ \mathrm{kg/m^3}$
Blood Heat Capacity	C_p	$3594\ \mathrm{J/K \cdot kg}$
Dynamic Viscosity	μ	$0.003\ \mathrm{N/m^2 s}$
Specific Heat Ratio in Blood	γ	1

(source: Hussain et al., [6])

To ensure the validity of the MATLAB script developed for simulating blood flow, a comparative simulation was conducted using Ansys Fluent 2024 R1 [28]. Ansys Fluent is a widely used CFD software for modeling fluid dynamics problems and is implemented with efficient and flexible data structures written in C language [30]. The blood flow in vessels affected by atherosclerosis was simulated in Fluent using the finite volume method, solving the governing Navier-Stokes equations with the same key physical parameters as listed in Table 1, including thermal conductivity (k), blood density (ρ), dynamic viscosity (μ), specific heat ratio (γ), and blood heat capacity (C_p). The parameter values presented in Table 1 are systematically incorporated into the set of governing Equation (1) through Equation (19) to generate the velocity and pressure profiles shown in Figure 3 to Figure 14. Geometric parameters, such as the percentage of stenosis, vessel length (L), and constriction depth (δ), define the spatial domain and boundary conditions, influencing equations that describe vessel geometry and stenosis shape. Fluid properties like blood density (ρ) and viscosity (μ) are applied within the Navier–Stokes momentum equations to capture the flow behavior, particularly affecting viscous stress terms that determine velocity gradients and pressure drops. Flow parameters such as the inlet velocity (u_{avg}) serve as boundary conditions in the velocity and pressure equations, setting the initial and exit flow conditions. The resistance coefficient ($\hat{R}$), which characterizes stenosis-induced flow resistance, is integrated into specific equations modeling pressure gradients. Additionally, spatial variables, including the position along the vessel (z) and stenosis location (h) modulate local velocity and pressure changes along the arterial length. Together, these parameter values, when input into their respective equations, allow the numerical solution to capture the complex hemodynamic changes across different degrees of vessel constriction, resulting in the velocity and pressure distributions depicted in Figure 3 through Figure 14.

Validation of the MATLAB script was performed by quantitatively comparing key output parameters such as velocity profiles and pressure distributions against those obtained from Fluent simulations, a widely recognized CFD software that employs the finite volume method for fluid flow modeling. The primary validation criteria included percentage error and root mean square error (RMSE) calculated at critical points within the vessel domain. A threshold error of less than 5% was set as the acceptable limit to confirm the accuracy and reliability of the MATLAB model. This quantitative approach provides an objective measure to assess the fidelity of the MATLAB simulation in replicating the more established Fluent results. Despite minor discrepancies caused by differences in numerical methods and model assumptions, the comparison demonstrated overall consistency, thereby ensuring the validity of the MATLAB-based blood flow simulation.

3. RESULTS AND DISCUSSION

The visualization results generated from the MATLAB program are graphs of blood flow velocity and pressure in narrowed blood vessels, which can be seen in Figure 3 – Figure 14. Using MATLAB, we simulated blood flow through vessels narrowed by 30 %, 50 %, and 70 % of their original diameter to observe how stenosis thickness alters velocity; inlet speeds of 0.3, 0.4, and 0.5 m/s (numerically calibrated to 0.27, 0.32, and 0.37 m/s) were applied, and the resulting graph plots velocity along a 25 mm domain, with blue, green, and red lines distinguishing each inlet speed, showing that tighter constrictions raise local peak velocity while post-stenosis sections slow more uniformly, and clear titles, axis labels, legends, and a dashed grid enhance readability.

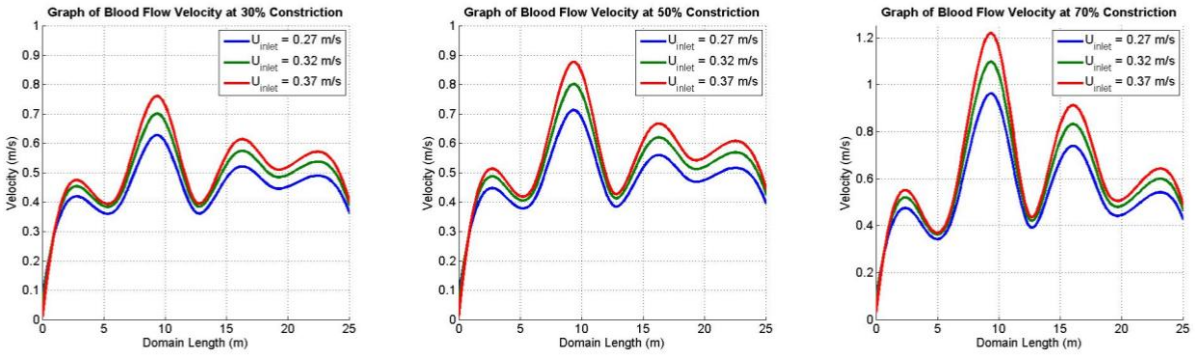

(a) (b) (c)

Figure 3. Graph of Blood Flow Velocity Based on Initial Velocity at (a) 30%, (b) 50%, and (c) 70% Constriction

Figure 3 is a velocity graph with blue, green, and red colored lines representing initial velocities of 0.27 m/s, 0.32 m/s, and 0.37 m/s, respectively. At the highest initial velocity of 0.37 m/s, the blood velocity exceeds the normal flow velocity. **Figure 3** (a) shows the blood flow velocity at 30% constriction, with peak velocities of 0.62854 m/s (blue), 0.70169 m/s (green), and 0.76133 m/s (red). **Figure 3** (b) shows the velocity at 50% constriction with peak values of 0.713793 m/s (blue), 0.802734 m/s (green), and 0.878161 m/s (red). **Figure 3** (c) presents the velocity at 70% constriction, where the blue, green, and red graphs reach 0.96314 m/s, 1.098257 m/s, and 1.21986 m/s, respectively. This data clearly demonstrates that the greater the initial velocity of blood flow, the higher the velocity in the narrowed area, which then decreases after passing through the constricted section. This behavior is consistent with fluid dynamics principles, where velocity increases to maintain volumetric flow rate through reduced cross-sectional areas. Therefore, **Figure 3** empirically and systematically confirms the positive correlation between initial blood velocity and blood flow velocity in constricted arteries, supporting the proposed hypothesis.

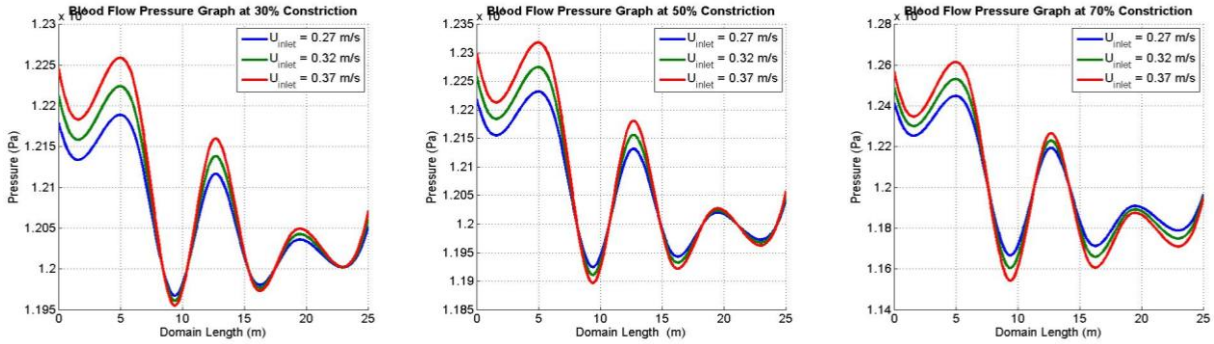

(a) (b) (c)

Figure 4. Blood Flow Pressure Graph Based on Initial Velocity at (a) 30%, (b) 50%, and (c) 70% Constriction

Figure 4 shows that the blood flow pressure graph at each constriction has decreased. **Figure 4** (a) shows the blood flow pressure graph at 30% constriction. The blue graph shows the lowest result of blood flow pressure of 11967.1 Pa, the green graph 11961 Pa, and the red graph 11954.9 Pa. **Figure 4** (b) shows the blood flow pressure graph at 50% constriction. The blue graph shows the lowest blood flow pressure of 11924.55 Pa, the green graph 11910.57 Pa, and the red graph 11896.6 Pa. **Figure 4** (c) shows the blood flow pressure graph at 70% constriction. The blue graph shows the lowest result of blood flow pressure of 11665.8 Pa, the green graph shows 11603.9 Pa, and the red graph shows 11542 Pa. This shows that the greater the initial velocity of blood flow, the lower the blood flow pressure in the constriction area.

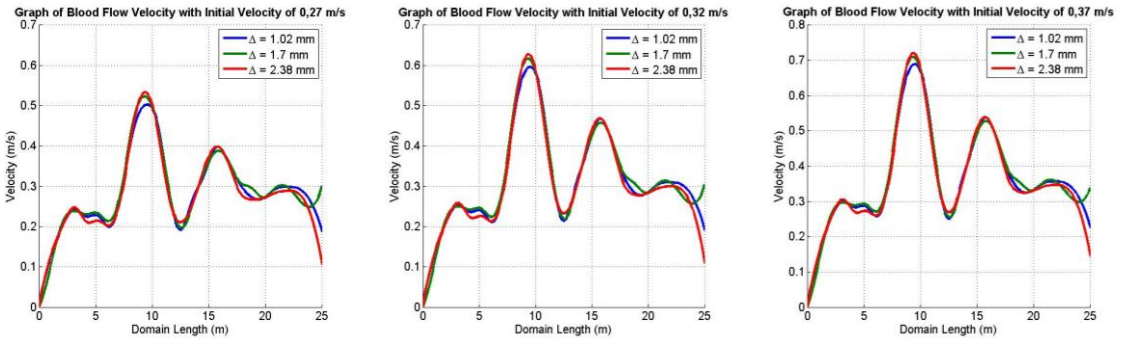

(a) (b) (c)

Figure 5. Graph of Blood Flow Velocity Based on the Amount of Constriction at an Initial Velocity of (a) 0.27 m/s, (b) 0.32 m/s, and (c) 0.37 m/s

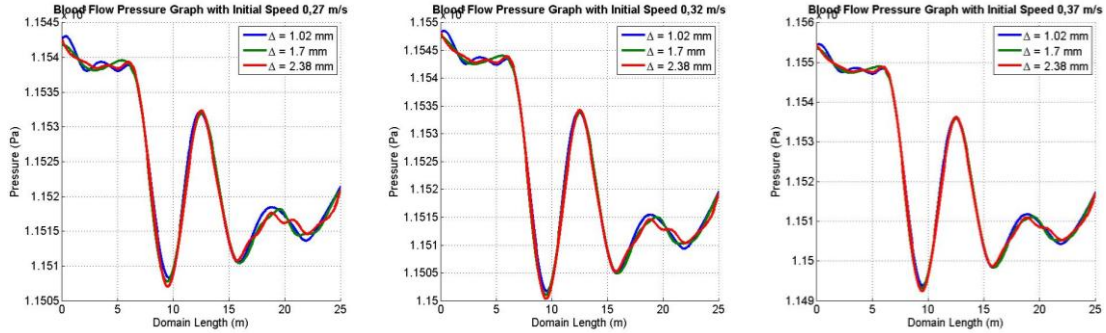

(a) (b) (c)

Figure 6. Blood Flow Pressure Graphs Based on the Amount of Constriction at an Initial Velocity of (a) 0.27 m/s, (b) 0.32 m/s, and (c) 0.37 m/s

Table 2. Blood Flow Velocity and Pressure from MATLAB

Initial Velocity (m/s)	Constriction	Highest Velocity (m/s)	Lowest Pressure (Pa)
0.27	30%	0.501001	11508.59
	50%	0.522543	11507.77
	70%	0.533427	11507.11
0.32	30%	0.59494	11501.9
	50%	0.61648	11501.1
	70%	0.62736	11500.4
0.37	30%	0.68833	11493.9
	50%	0.70987	11493.1
	70%	0.72075	11492.4

Figure 5 shows that increasing the initial blood-flow velocity from 0.27 m/s to 0.37 m/s elevates the peak velocity along the vessel, particularly at the constricted sections around 5 m and 15 m. Differences in narrowing (Δ = 1.02 mm, 1.7 mm, and 2.38 mm) influence the velocity distribution: greater constriction tends to yield slightly higher peak speeds, reaching about 0.72075 m/s at certain points. The consistent velocity patterns across all three degrees of narrowing indicate a stable simulation and clearly illustrate how stenosis markedly accelerates blood flow.

Figure 6 presents blood-flow pressure profiles for three inlet velocities, 0.27 m/s, 0.32 m/s, and 0.37 m/s, combined with stenosis lengths (Δ) of 1.02 mm, 1.7 mm, and 2.38 mm. A pronounced pressure drop appears at roughly 10 m along the domain, pinpointing the site of vascular narrowing. In **Figure 6** (c), this decline becomes steeper, reaching 11492.4 Pa as the inlet velocity increases. Variations in stenosis length exert only a minor influence on the pressure pattern, because the curves for all three Δ values nearly overlap at every velocity. These results indicate that inlet velocity has a far more dominant effect on pressure changes than the range of stenosis lengths examined.

The blood flow velocity comparison graph between MATLAB and Ansys Fluent in the elliptical blood vessel constriction area can be seen in **Figure 7** - **Figure 8**.

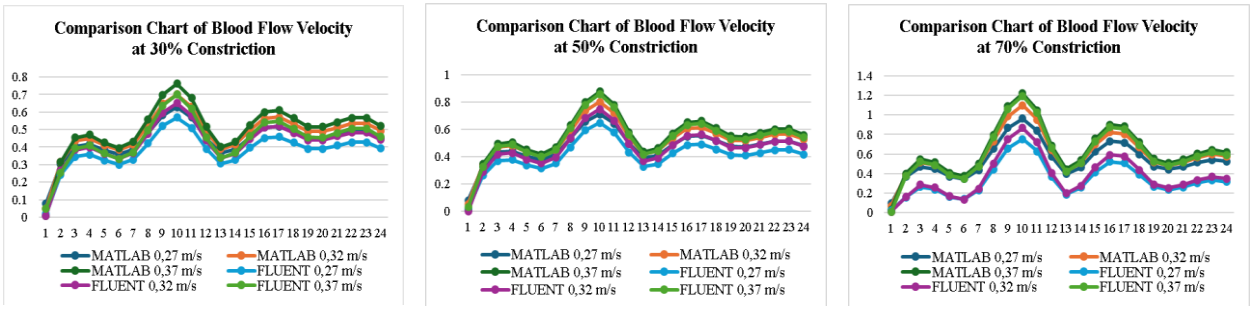

(a) (b) (c)

Figure 7. Comparison Graph of Blood Flow Velocity Between MATLAB and Ansys Fluent Based on Initial Velocity at Constriction (a) 30%, (b) 50%, and (c) 70%

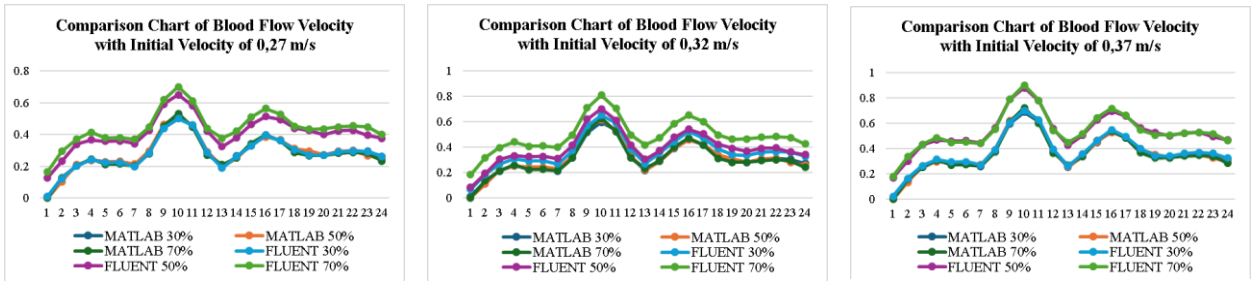

(a) (b) (c)

Figure 8. Comparison Graph of Blood Flow Velocity between MATLAB and Ansys Fluent Based on the Amount of Constriction at an Initial Velocity of (a) 0.27 m/s, (b) 0.32 m/s, and (c) 0.37 m/s

Figure 7 compares blood-flow velocities for arterial stenoses of 30 %, 50 %, and 70 % simulated with MATLAB and ANSYS Fluent at three inlet velocities (0.27 m/s, 0.32 m/s, and 0.37 m/s). Blood velocity rises with the degree of narrowing, and the highest peak appears at 70 % stenosis. MATLAB and Fluent generate closely matching trends, although minor point-by-point differences occur, demonstrating that the MATLAB model reliably reproduces Fluent's predictions of flow behaviour in a constricted artery. In general, greater stenosis leads to faster flow, highlighting acceleration caused by the narrowing.

Figure 8 presents blood-flow velocity profiles obtained with MATLAB and ANSYS Fluent for the same stenosis levels (30 %, 50 %, 70 %) and inlet velocities (0.27 m/s, 0.32 m/s, 0.37 m/s). Across all three plots, velocity increases as the percentage of narrowing grows, with the highest values typically recorded at 70 % stenosis. Fluent tends to report slightly higher velocities than MATLAB, particularly at severe constrictions. Raising the inlet velocity from 0.27 m/s to 0.37 m/s elevates velocities along the entire measurement domain. Both tools reproduce an almost identical velocity-variation pattern, confirming their consistency in modelling stenosis effects.

Figure 9 illustrates velocity fields for a 30 % stenosis at inlet velocities of (a) 0.27 m/s, (b) 0.32 m/s, and (c) 0.37 m/s. In panel (c), the higher inlet speed produces a pronounced velocity surge within the narrowed zone, shown by the color transition from yellow-green to red. The local peak rises by roughly 0.7 m/s as the flow passes through the constriction, which may impose greater pressure and shear on the vessel wall. The lower images originate from ANSYS Fluent, while the upper images come from an independent numerical model that yields a similar velocity pattern, thereby reinforcing the validity of the simulation results. **Figure 10** illustrates a blood-flow velocity simulation in an artery with 50 % stenosis for three inlet velocities: (a) 0.27 m/s, (b) 0.32 m/s, and (c) 0.37 m/s. The visualization reveals that higher inlet velocities concentrate greater flow speeds inside the narrowed segment, shown by deeper red hues. A higher inlet velocity accelerates and intensifies blood flow in the stenotic zone, potentially increasing turbulence and wall shear stress. Raising the inlet velocity from 0.27 m/s to 0.37 m/s produces a marked rise in local velocity up to 0.88 m/s in the 50 % stenosis, which correspondingly heightens the mechanical load on the vessel wall.

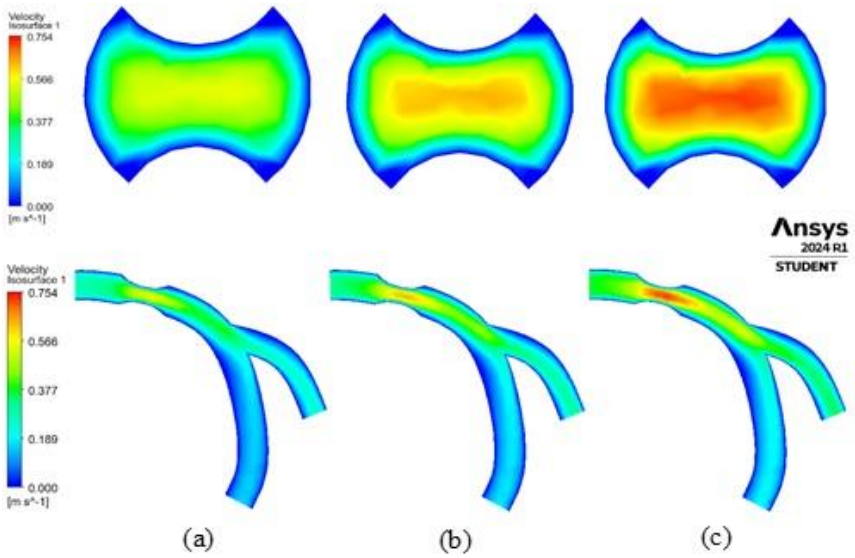

Figure 9. Simulation of Blood Flow Velocity at 30% Constriction with Initial Velocity of (a) 0.27 m/s, (b) 0.32 m/s, and (c) 0.37 m/s

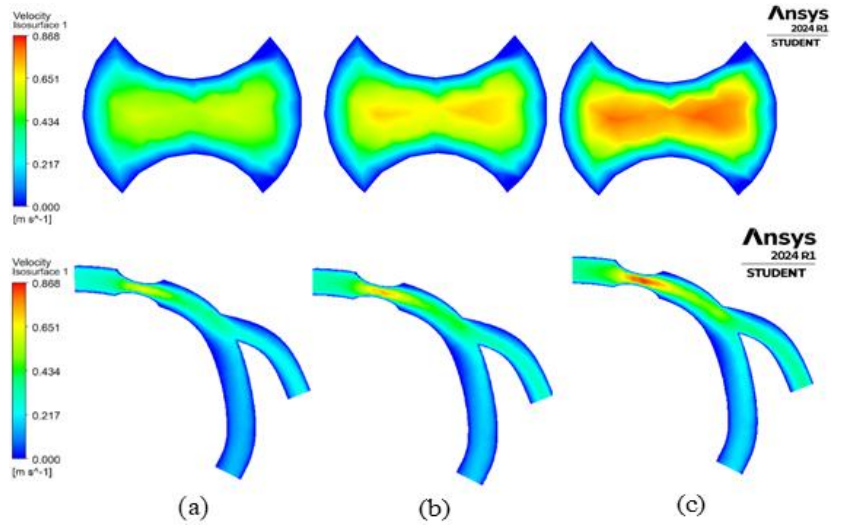

Figure 10. Simulation of Blood Flow Velocity at 50% Constriction with Initial Velocity of (a) 0.27 m/s, (b) 0.32 m/s, and (c) 0.37 m/s

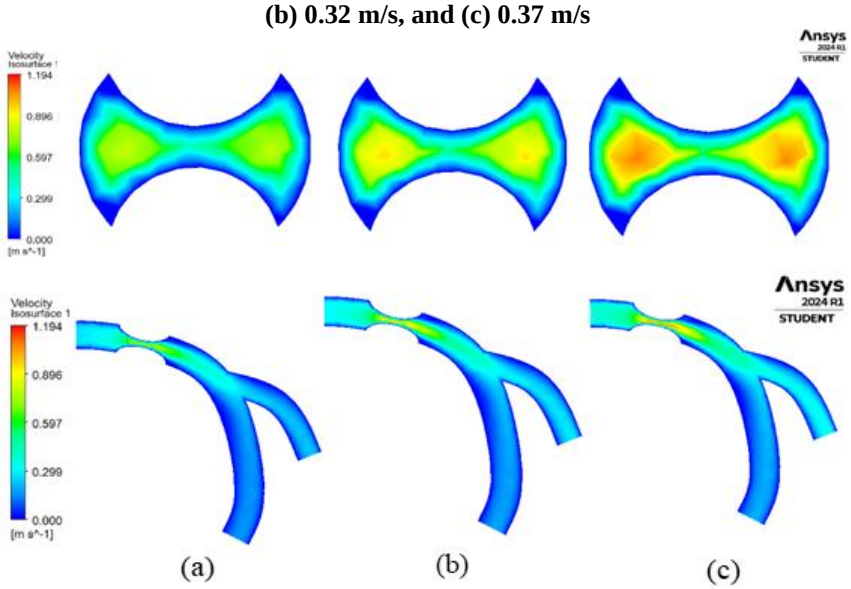

Figure 11. Simulation of Blood Flow Velocity at 70% Constriction with Initial Velocity of (a) 0.27 m/s, (b) 0.32 m/s, and (c) 0.37 m/s

Figure 11 presents a blood-flow velocity simulation for an artery with 70 % stenosis at the same inlet conditions: (a) 0.27 m/s, (b) 0.32 m/s, and (c) 0.37 m/s. The results confirm that higher inlet velocities further amplify flow speed in the constricted segment, evidenced by increasingly intense red coloration. In **Figure 11** (c), the velocity within the narrowed region reaches roughly 0.9 m/s, displayed as a more concentrated and sharper red band. These findings demonstrate that severe stenosis magnifies local blood acceleration as the inlet velocity rises.

Furthermore, the maximum speed at each constriction is shown in **Table 3** as follows.

Table 3. Blood Flow Velocity from Ansys Fluent

Initial Velocity (m/s)	Narrowing	Highest Velocity (m/s)
0.27	30%	0.5
	50%	0.651
	70%	0.7
0.32	30%	0.65
	50%	0.7
	70%	0.8
0.37	30%	0.7
	50%	0.88
	70%	0.9

The simulation results show that the more the blood vessels narrow, the higher the blood flow velocity. Of the three narrowings that have the potential to experience the most severe atherosclerosis disease, namely, blood vessels that experience 70% narrowing.

In **Figure 12**, which represents 30% stenosis, raising the inlet velocity from 0.27 m/s to 0.32 m/s and then to 0.37 m/s progressively amplifies the wall-pressure gradient: the high-pressure red-to-yellow zone, peaking at 12245.9 Pa, widens and shifts upstream of the constriction, while the lower-pressure blue-to-green region downstream, centered around 11954.9 Pa, remains dominant. This trend reveals an almost linear relationship between inlet velocity and arterial-wall pressure load, implying that greater flow rates can increase the likelihood of wall damage in the narrowed segment.

Figure 13 illustrates the 50 % stenosis scenario, where the pressure surge exceeds that of the 30% case: a red-to-orange zone upstream of the lesion peaks at approximately 12300 Pa. Even at an inlet velocity of 0.27 m/s, the arterial wall experiences a steep pressure gradient, and raising the velocity to 0.32 m/s and 0.37 m/s expands this high-pressure region while intensifying the downstream pressure drop to about 11896 Pa. Together, these findings show that both greater stenosis severity and higher flow rates impose heavier hemodynamic loads, potentially accelerating wall dysfunction in the narrowed arterial segment.

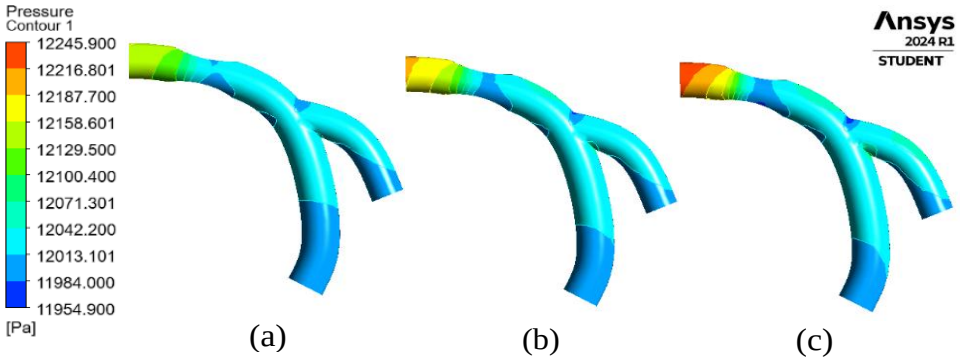

Figure 12. Simulation of Blood Flow Pressure at 30% Narrowing with Initial Velocity of (a) 0.27 m/s, (b) 0.32 m/s, and (c) 0.37 m/s

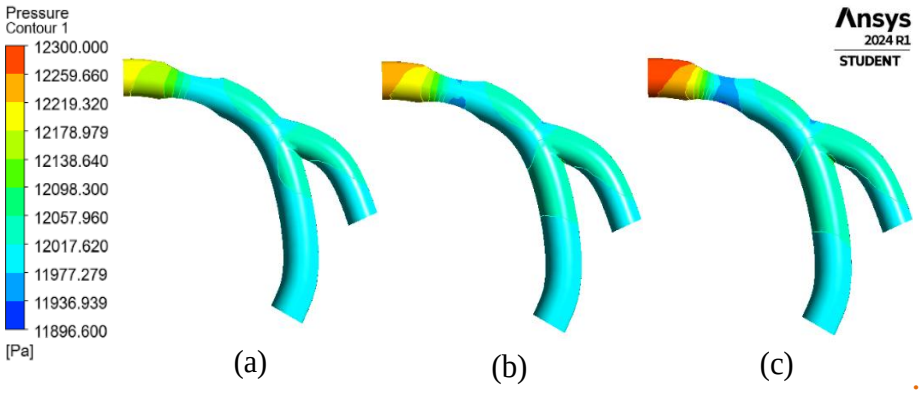

Figure 13. Simulation of Blood Flow Pressure at 50% Narrowing with Initial Velocity of (a) 0.27 m/s, (b) 0.32 m/s, and (c) 0.37 m/s

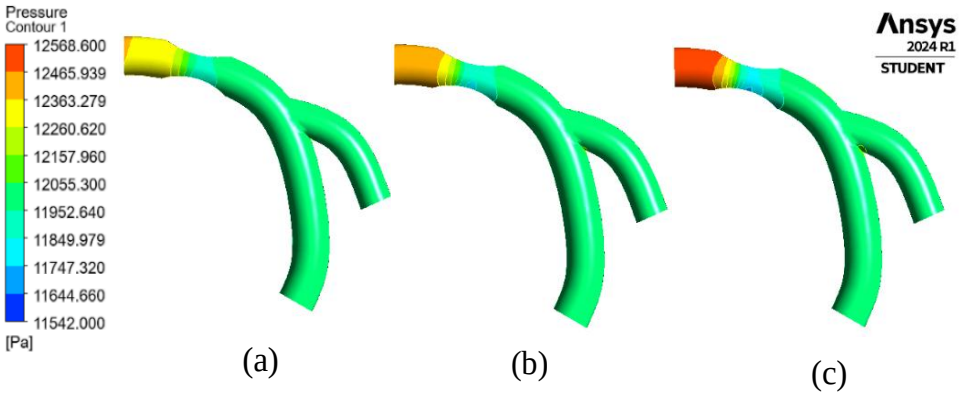

Figure 14. Simulation of Blood Flow Pressure at 70% Narrowing with Initial Velocity of (a) 0.27 m/s, (b) 0.32 m/s, and (c) 0.37 m/s

Figure 14 demonstrates that a 70 % stenosis produces the steepest pressure surge compared with the 30 % and 50 % cases. At an inlet velocity of 0.27 m/s (**Figure 14** (a)), only a thin yellow band of 12568.6 Pa appears upstream of the stenosis, whereas the downstream wall has already fallen into the green-blue zone at 11747.32 Pa. Raising the velocity to 0.32 m/s (**Figure 14** (b)) and 0.37 m/s (**Figure 14** (c)) expands the red-orange region with a peak pressure of approximately 12568.6 Pa farther upstream, so the pressure gradient across the stenosis becomes progressively steeper. These findings indicate that the combination of severe narrowing and high flow rate maximizes the pressure differential, thereby heightening the risk of vessel-wall injury within the constricted zone.

Table 4. Maximum Velocity based on the Same Initial Velocity

Narrowing	Initial Velocity (m/s)	Maximum Velocity in MATLAB (m/s)	Maximum Velocity in Ansys Fluent (m/s)
30%	0.27	0.62854	0.566
	0.32	0.70169	0.651
	0.37	0.76133	0.7
50%	0.27	0.713793	0.65
	0.32	0.802731	0.75
	0.37	0.878161	0.86
70%	0.27	0.96314	0.754
	0.32	1.098257	0.868
	0.37	1.21986	1.194

Table 4 shows that peak flow velocity rises in tandem with both inlet velocity and stenosis severity. In the 30 % narrowing, increasing the inlet velocity from 0.27 m/s to 0.32 m/s elevates the maximum velocity from 0.628 m/s to 0.761 m/s in MATLAB and from 0.566 m/s to 0.700 m/s in Fluent. A similar-but more pronounced-trend appears at 50 % stenosis: an inlet range of 0.27-0.37 m/s yields peak velocities of 0.713-0.878 m/s (MATLAB) and 0.650-0.860 m/s (Fluent). The most dramatic effect occurs at 70 % stenosis, where an inlet velocity of 0.27 m/s triggers peak values of 0.963 m/s (MATLAB) and 0.754 m/s (Fluent), then climbs to roughly 1.22 m/s and 1.194 m/s at 0.37 m/s. Throughout, MATLAB predicts slightly higher peaks

than Ansys Fluent, yet both tools consistently confirm a positive link between greater inlet velocity, higher degrees of narrowing, and larger maximum blood velocities.

Table 5. Maximum Speed based on Same Narrowing Size

Initial Velocity (m/s)	Narrowing	Maximum Velocity in MATLAB (m/s)	Maximum Velocity in Ansys fluent (m/s)
0.27	30%	0.501001	0.5
	50%	0.522543	0.651
	70%	0.533427	0.7
0.32	30%	0.59494	0.65
	50%	0.61648	0.7
	70%	0.62736	0.8
0.37	30%	0.68833	0.7
	50%	0.70987	0.88
	70%	0.72075	0.9

Table 5 reinforces this dual pattern: increasing either stenosis severity or initial velocity raises the peak flow velocity. At an inlet velocity of 0.27 m/s, Fluent reports a rise from 0.500 m/s (30 %) to 0.700 m/s (70 %), whereas MATLAB shows a more moderate climb from 0.500 m/s to 0.533 m/s. Similar behaviour occurs at 0.32 m/s and 0.37 m/s, where Fluent indicates increases of roughly 0.15-0.20 m/s for every additional 20 % narrowing. Method-to-method differences remain minor in mild stenoses but widen to about $\pm$0.18 m/s at 70 %, suggesting that Fluent predicts a more aggressive acceleration as the lumen narrows further. Overall, both simulations agree that peak velocity scales positively with inlet speed and stenosis severity, although Fluent systematically provides the higher estimates, especially under severe narrowing.

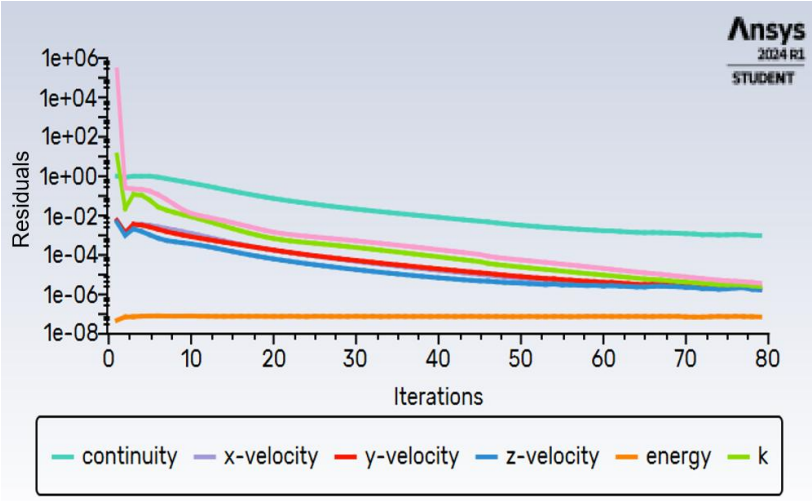

Figure 15. Scaled Residual Graph

Figure 15 shows the scaled residual graph from Ansys Fluent software. The scaled residual graph shows the convergence, where the iteration will stop if it has converged. **Figure 15** shows the simulation of blood flow that is narrowed by 30%, 50%, and 70% has a convergent iteration characterized by the value getting closer to zero.

4. CONCLUSION

This study has conducted a numerical analysis of blood vessel constriction due to atherosclerosis disease using the finite volume method. It has examined how varying degrees of constriction influence the hemodynamic characteristics within the affected blood vessels. The study also validates a mathematical model of blood flow through stenotic arteries over a broad range of stenosis levels, from 30% to 70%. The detailed findings from this study are presented below:

- The study reveals that when the luminal reduction in coronary arteries exceeds 50%, haemodynamic stresses increase significantly. At 70% stenosis, these stresses surpass physiological safety margins, heightening the risk of endothelial damage and plaque rupture. Peak centre-line speeds rose from

approximately 0.63 m/s in the 30% model to 1.22 m/s in the 70% model, while the corresponding pressure drops increased from about 8 kPa to more than 11 kPa.

- The custom MATLAB solver provides accurate results compared to the ANSYS Fluent model, with a deviation of no more than 7%. Convergence was achieved in fewer than 145 SIMPLE iterations, with residuals below 1×10^{-4}, making it a fast and cost-effective alternative for simulations. This solver offers a rapid screening tool for clinicians and researchers.
- The current model's assumptions—rigid walls, axisymmetry, steady flow, and Newtonian viscosity—must be relaxed in future work. To improve accuracy for cardiovascular risk assessment, arterial compliance, pulsatile inflow, non-Newtonian rheology, and patient-specific geometries should be incorporated into the model.

For future research, the authors suggest exploring the following potential areas:

- Patient-Specific Geometries**:** Incorporating patient-specific geometries will enhance the clinical relevance of the model.
- Fluid-Structure Interaction**:** Including fluid-structure interaction in the model is essential to account for arterial elasticity.
- Realistic Pulsatile Inflow Waveforms: Applying realistic pulsatile inflow waveforms will help simulate more accurate physiological conditions.
- Benchmarking Against Experimental Data: Future work should compare the model's results against laboratory measurements or clinical imaging to ensure accuracy and reliability.
- Expanding Model Complexity: The model should be extended to evaluate non-Newtonian rheology under varying hematocrit levels and explore the impact of multi-lesion configurations, further improving its clinical relevance.

AUTHOR CONTRIBUTIONS

Arif Fatahillah: Conceptualization, Methodology, Software, Supervision, Writing - Original Draft, Validation. Umi Mubarokah: Formal Analysis, Data Curation, Visualization, Writing – Review and Editing. Rafiantika Megahnia Prihandini: Investigation, Methodology, Software. Edy Wihardjo: Resources, Project Administration, Funding Acquisition, Software. Robiatul Adawiyah: Software, Validation, Writing – Review and Editing. Saddam Hussen: Visualization, Formal Analysis, Writing – Review and Editing. Lioni Anka Monalisa: Supervision, Project Administration, Writing – Review and Editing. All authors discussed the results and contributed to the final manuscript.

FUNDING STATEMENT

This research received no specific grant from any funding agency in the public, commercial, or not-for-profit sectors.

ACKNOWLEDGMENT

We sincerely thank the Mathematics Education Study Program, Faculty of Teacher Training and Education, University of Jember, for the valuable knowledge and continuous support. We also extend our heartfelt appreciation to the Mathcome Research Group for the facilities and assistance provided throughout this work.

DECLARATION

The authors declare that they have no competing interests and no conflicts of interest to disclose in connection with this research.

REFERENCES

[1] M. A. Hussain, A. Al Mamun, S. A. E. Peters, M. Woodward, and R. R. Huxley, "THE BURDEN OF CARDIOVASCULAR DISEASE ATTRIBUTABLE TO MAJOR MODIFIABLE RISK FACTORS IN INDONESIA," *J Epidemol*, vol. 26, no. 10. pp. 515–521, 2016, doi: https://doi.org/10.2188/jea.JE20150178.

[2] M. Soleimani, B. Dashtbozorg, M. Mirkhalaf, and S. M. Mirkhalaf, "A MULTIPHYSICS-BASED ARTIFICIAL NEURAL NETWORKS MODEL FOR ATHEROSCLEROSIS," *Heliyon*, vol. 9, no. 7, p. e17902, 2023, doi: https://doi.org/10.1016/j.heliyon.2023.e17902.

[3] W. Chen, Z. Li, Y. Zhao, Y. Chen, and R. Huang, "GLOBAL AND NATIONAL BURDEN OF ATHEROSCLEROSIS FROM 1990 TO 2019: TREND ANALYSIS BASED ON THE GLOBAL BURDEN OF DISEASE STUDY 2019," *Chin. Med. J. (Engl).*, vol. 136, no. 20. pp. 2442–2450. 2023, doi: https://doi.org/10.1097/CM9.0000000000002839.

[4] F. Anita, B. Antoro, and S. Barokah, "PENERAPAN SENAM ERGONOMIK TERHADAP PENURUNAN TEKANAN DARAH LANSIA PENDERITA HIPERTENSI," *Media Husada J. Nurs. Sci.*, vol. 4, no. 2, 2023, doi: https://doi.org/10.57218/jkj.Vol2.Iss2.789.

[5] L. F. Tampubolon, A. Ginting, and F. E. S. Turnip, "GAMBARAN FAKTOR YANG MEMPENGARUHI KEJADIAN PENYAKIT JANTUNG KORONER (PJK) DI PUSAT JANTUNG TERPADU (PJT)," *J. Ilm. Permas J. Ilm. STIKES Kendal*, vol. 13, no. 3, pp. 1043–1052, 2023, doi: https://doi.org/10.32583/pskm.v13i3.1077.

[6] A. Hussain, M. Naveel, R. Dar, W. Khalid, and E. M. Tag-eldin, "NUMERICAL SIMULATION OF UNSTEADY GENERIC NEWTONIAN BLOOD FLOW AND HEAT TRANSFER THROUGH DISCREPANT SHAPED DILATABLE ARTERIAL STENOSIS," *Results Eng.*, vol. 18, no. May, p. 101189, 2023, doi: https://doi.org/10.1016/j.rineng.2023.101189.

[7] A. Maharani, Sujarwoto, D. Praveen, D. Oceandy, G. Tampubolon, and A. Patel, "CARDIOVASCULAR DISEASE RISK FACTOR PREVALENCE AND ESTIMATED 10-YEAR CARDIOVASCULAR RISK SCORES IN INDONESIA : THE SMARTHEALTH EXTEND STUDY," *PLoS One*, vol. 14, no. 4, pp. 1–13, 2019, doi: https://doi.org/10.1371/journal.pone.0215219.

[8] A. Szpicer *et al.*, "INNOVATIVE IMPLEMENTATION OF COMPUTATIONAL FLUID DYNAMICS IN PROTEINS DENATURATION PROCESS PREDICTION IN GOOSE BREAST MEAT AND HEAT-TREATMENT PROCESSES OPTIMIZATION," *Appl. Sci.*, vol. 14, no. 13, pp. 1–22, 2024, doi: https://doi.org/10.3390/app14135567.

[9] A. G. Rahma, K. Yousef, and T. Abdelhamid, "BLOOD FLOW CFD SIMULATION ON A CEREBRAL ARTERY OF A STROKE PATIENT," *SN Appl. Sci.*, vol. 4, no. 10. 2022, doi: https://doi.org/10.1007/s42452-022-05149-y.

[10] M. Madaliev *et al.*, "THE EFFECT OF SLIP ON THE DEVELOPMENT OF FLOW SEPARATION DUE TO A BUMP IN A CHANNEL BASED ON A TWO-FLUID TURBULENCE MODEL," *E3S Web Conf.*, vol. 508, 2024, doi: https://doi.org/10.1051/e3sconf/202450806003.

[11] H. K. Versteeg and W. Malalasekera, "AN INTRODUCTION TO COMPUTATIONAL FLUID DYNAMICS," 2nd ed., Harlow, England: Pearson Education Limited, 2007.

[12] A. Fatahillah, A. D. Pratiwi, S. Setiawani, A. I. Kristiana, and R. Adawiyah, "NUMERICAL ANALYSIS IN ARTERIAL STENOSIS AFFECTED BY ISCHEMIC HEART DISEASE USING FINITE VOLUME METHOD," *BAREKENG J. Ilmu Mat. dan Terap.*, vol. 18, no. 1, pp. 0179–0192, 2024, doi: https://doi.org/10.30598/barekengvol18iss1pp0179-0192.

[13] N. Georgieva, S. Delcheva, and P. Tsankov, "ANALYSIS OF THE CAPABILITIES OF SOFTWARE PRODUCTS TO SIMULATE THE BEHAVIOR OF DYNAMIC FLUID FLOWS," *IOP Conf. Ser. Mater. Sci. Eng.*, vol. 1031, no. 1, 2021, doi: https://doi.org/10.1088/1757-899X/1031/1/012079.

[14] R. Shoufiah and S. Nuryanti, *FAKTOR-FAKTOR PENENTU KUALITAS HIDUP PASIEN JANTUNG KORONER*. Yogyakarta, Indonesia: CV. Jejak Pustaka, 2022.

[15] S. S. Narayan, S. Saha, A. Bhattacharjee, M. I. Khan, F. Zouidi, and S. M. Eldin, "ASSESSING THE IMPACT OF HYPERVISCOSITY ON STENOSIS SHAPE IN COVID PATIENTS," *Ain Shams Eng. J.*, vol. 14, no. 12, p. 102227, 2023, doi: https://doi.org/10.1016/j.asej.2023.102227.

[16] L. Bachtiar, R. A. Gustaman, and S. Maywati, "Faktor risiko yang berhubungan dengan kejadian penyakit jantung koroner (PJK)," vol. 19, no. 1, pp. 52–60. 2023, doi: 10.37058/jkki.v19i1.6862.

[17] A. Hussain, M. N. Riaz Dar, W. K. Cheema, E. M. Tag-eldin, dan R. Kanwal, "Numerical simulation of unsteady generic Newtonian blood flow and heat transfer through discrepant shaped dilatable arterial stenosis," *Results in Engineering*, vol. 18, 2023, doi: 10.1016/j.rineng.2023.101189.

[18] H. Gao, J. Zhang, H. Li, and X. Zhang, "Hemodynamic analysis of stenosed arteries using computational fluid dynamics," *Appl. Sci.*, vol. 10, no. 8, p. 2923, 2020, doi: 10.3390/app10082923.

[19] Y. Zhang, J. Wu, and K. Xu, "Numerical simulation of blood flow in stenosed arteries with non-Newtonian fluid model," *Int. J. Numer. Meth. Biomed. Eng.*, vol. 34, no. 4, p. e2948, 2018, doi: 10.1002/cnm.2948.

[20] U. Morbiducci, R. Ponzini, G. Rizzo, and A. Redaelli, "Hemodynamics and atherosclerosis: Insights and perspectives from computational studies," *Curr. Vasc. Pharmacol.*, vol. 11, no. 4, pp. 552–569, 2013, doi: 10.2174/1570161111311040004.

[21] I. P. Widiarta, M. Suarda, M. Sucipta, and I. G. K. Sukadana, "Simulasi CFD pertukaran udara di ruang tindakan klinik kesehatan," *J. METTEK*, vol. 8, no. 2, p. 83, 2022, doi: 10.24843/mettek.2022.v08.i02.p03.

[22] MATLAB, version R2013a, The MathWorks Inc., Natick, Massachusetts, 2013.

[23] J. WANG, "The application of matlab in the mathematics teaching of computer majors," *Scalable Comput.*, vol. 25, no. 4, pp. 2916–2933, 2024, doi: 10.12694/scpe.v25i4.2889.

[24] A. Fatahillah, M. Jannah, S. Setiawani, T. B. Setiawan, and A. I. Kristiana, "Numerical analysis of airflow in trachea affected by thyroid cancer using finite volume method," *CAUCHY J. Mat. Murni dan Apl.*, vol. 9, no. 1, pp. 82–93, 2024, doi: 10.18860/ca.v9i1.24376.

[25] S. Y. J. Prasetyo, "Metode Penelitian Penginderaan Jauh," [Online]. Tersedia: https://scholar.google.com/scholar?hl=id&as_sdt=0%2C5&q=+sri+yulianto+joko+prasetyo+Metode+Penelitian+Penginderaan+Jauh&btnG=, diakses Jan. 20, 2024.

[26] I. Junaedi *et al*., *Manifestasi Kurikulum Luar*, CV. Zenius Publisher, 2022. [Online]. Tersedia: https://www.google.co.id/books/edition/MANIFESTASI_KURIKULUM_LUAR_NEGERI/NR2HEAAAQBAJ?hl=id&gbpv=1&dq=Manifestasi+Kurikulum+Luar&pg=PT92&printsec=frontcover, diakses Feb. 25, 2024.

[27] S. S. Lim, S. Park, B. H. Oh, K. Jung, J. W. Bae, dan D. H. Bae, "RNF213 vasculopathy manifested in various forms within a family: A case report," *Medicine (United States)*, vol. 102, no. 50. p. e36627, 2023, doi: 10.1097/MD.0000000000036627.

[28] ANSYS®, *ANSYS Fluent User's Guide*, Release 2024 R1, Student Version, ANSYS, Inc., Canonsburg, PA, USA, 2024.

[29] M. Roy, B. S. Sikarwar, M. Bhandwal, and P. Ranjan, "Modelling of blood flow in stenosed arteries," *Procedia Comput. Sci.*, vol. 115, pp. 821–830. 2017, doi: 10.1016/j.procs.2017.09.164.

[30] A. Fatahillah, M. U. Nuha, and S. Setiawani, "Analisis numerik aliran udara pada rongga hidung akibat penyakit sinusitis menggunakan metode volume hingga," *Limits J. Math. Its Appl.*, vol. 19, no. 2, pp. 217–227, 2022, doi: 10.12962/limits.v19i2.13683.